Demographic variability and heterogeneity among individuals within and among clonal bacteria strains

Lionel Jouvet[1,2], Alexandro Rodríguez-Rojas[3], Ulrich K. Steiner[1,2*]

[1] Max-Planck Odense Centre on the Biodemography of Aging, Campusvej 55, 5230 Odense, Denmark

[2] Biology Department, University of Southern Denmark, Campusvej 55, 5230 Odense, Denmark

[3] Institute of Biology, Freie Universität Berlin, Königin-Luise-Straße 1-3, 14195 Berlin, Germany

Alexandro Rodríguez-Rojas: ORCID iD: 0000-0002-4119-8127

*corresponding author: usteiner@biology.sdu.dk; orcid.org/0000-0002-1778-5989

This submission includes Supplementary material

Data deposition

The processed image analysis data as well as the Leslie matrices will be archived at Dryad.org.

Keywords: fixed heterogeneity, dynamic heterogeneity, neutral variability, trade-off, life history evolution, senescence, aging.

Abstract

Identifying what drives individual heterogeneity has been of long interest to us ecologists, evolutionary biologists and biodemographers, because only such identification provides deeper understanding of ecological and evolutionary population dynamics. In natural populations we are challenged to accurately decompose the generating genetically fixed and selectively neutral dynamic moments of heterogeneity. Rather than working on wild populations we present here data from a simple bacterial system in the lab, *Escherichia coli*. Our system, based on cutting-edge microfluidic techniques, provides high control over the genotype and the environment. Only such high control provides the means to unambiguously decompose and quantify fixed, genetic variability, and dynamic, stochastic variability among individual demographic components. We show that within clonal individual variability (neutral dynamic heterogeneity) in lifespan and lifetime reproduction is dominating at about 93-95%, over the 5-7% genetically (adaptive fixed) driven differences. The genetic differences among the clonal strains still lead to substantial variability in population growth rates (fitness), but the neutral variability slows adaptive change, by enhancing genetic drift, and lowering overall population growth. We also revealed a surprising diversity in demographic patterns among the clonal strains, which indicates diverse underlying stochastic cell-intrinsic processes that shape these demographic patterns. Such diversity is surprising since all cells belong to the same bacteria species, *E. coli*, and still exhibit patterns such as classical senescence, non-senescence, or negative senescence. We end by discussing whether similar levels of neutral variability might be detected in other systems and close by stating the open questions how such neutral heterogeneity is maintained, how it has evolved, and whether it is adaptive.

Heterogeneity among individuals has important ecological and evolutionary implications because it determines the pace of ecological and evolutionary adaptation and shapes eco-evolutionary feedbacks (Hartl and Clark 2007, Steiner and Tuljapurkar 2012, Vindenes and Langangen 2015). Despite substantial methodological and empirical efforts, we are still challenged to unambiguously differentiate the causes that drive the observed heterogeneity among individuals in their life courses, their traits, and their fitness components (Steiner and Tuljapurkar 2012, Bonnet and Postma 2016, Cam et al. 2016). We have consensus that heterogeneity among individuals is caused by changes in the environment, by variation in the genotype, by the genotype-by-environment interaction, and by noise or processes that show stochastic properties (Endler 1986, Finch and Kirkwood 2000, Kirkwood et al. 2005). The latter cause has either been deemed as noise associated with non-biological processes, e.g. measurement error, and with unknown hidden processes that were considered to be of little biological relevance. Alternatively, this "noise" has been investigated for underlying biological processes with stochastic characteristics. Numerous mechanisms of such "hidden" processes with stochastic properties have been identified including e.g. stochastic gene expression, protein folding and misfolding, and their potential cascading effects up to the organism level (Elowitz et al. 2002, Lindner and Demarez 2009, Balázsi et al. 2011, Ackermann 2015). Still, the link between such processes at the molecular or physiological level and the individual life courses is largely missing. This unexplained variability has also been of interest in quantitative and population genetics because it slows evolutionary dynamics by lowering heritabilities and enhancing genetic drift (Lande et al. 2003, Hartl and Clark 2007).

The challenge we face in decomposing the observed heterogeneity into its genetic, environmental, and stochastic component is heightened in natural populations. In such populations, we are confronted with high genetic diversity and complex environmental and gene-by-environment interactions (Fitzpatrick et

al. 2016). Our knowledge about the genotypes at the individual level is limited (e.g. pedigree) or in many cases totally absent. Certain environmental variables are usually known at the population level, but micro-environmental differences are less explored. The response of individuals to the known population level environmental factors varies – e.g. due to gene-by-environment interactions – and individuals are differently affected by the population level environment – e.g. not all individuals are exposed equally. In ecology, we are well aware that we cannot encompass the whole complexity of natural systems and hence the additional variance is seen as a combination of error and some sort of hidden drivers of heterogeneity. However, we still aim to identify the cause of this additional heterogeneity since only such identification allows forecasting of and understanding of evolutionary and ecological population dynamic processes (Lande et al. 2003, Tuljapurkar et al. 2009, Steiner et al. 2010).

Not only empirically are we challenged to decompose the observed variance in natural populations, also from a methodological point of view await us challenges. Various statistical approaches aim at classifying the hidden heterogeneity as either fixed at birth, e.g. additive genetic effects or maternal effects, or as dynamic heterogeneity, heterogeneity generated during the course of life (Tuljapurkar et al. 2009, Steiner et al. 2010, Steiner and Tuljapurkar 2012, Bonnet and Postma 2016, Cam et al. 2016). Such models, be they based on mixed effect models, Markov chains, hidden Markov chains, covariate models or related models, are biased and cannot reveal the accurate underlying mechanism unless the contributing factors and the underlying error structure is known (Bonnet and Postma 2016, Cam et al. 2016). This applies to both so-called neutral models that base their arguments on dynamic heterogeneity and adaptive selective models that base their arguments on fixed heterogeneity. Note, in the fixed type of models there remains a large unexplained variance of unknown origin.

In order to circumvent these empirical and methodological challenges we face in natural populations, we used here cutting-edge microfluidic technologies on a simple bacterial system in the lab, *Escherichia coli*. This system allowed us to unambiguously decomposing and quantify fixed, genetic variability and dynamic, stochastic variability among individuals. In comparing isogenic (clonal) individuals within and among seven (clonal) bacteria strains under highly controlled and constant environmental conditions we were able to unambiguously identify the genetic cause, i.e. fixed heterogeneity, and the stochastic cause, i.e. dynamic heterogeneity, behind the individual heterogeneity. Our system also excluded any environmental variability sharpening our focus on fixed selective and dynamic neutral heterogeneity. As expected, among strain genetic variability was modest compared to the substantial within strain variability in reproduction and survival. Variance in lifespan within strains explained ~94.4% and 5.6% was related to among strain variance in lifespan. Variance in lifetime reproductive success within strains explained ~93.2% and 6.8% was related to among strain variance. Our finding does not imply that the genetic variability is not relevant, it just highlights that there is large amount of neutral heterogeneity expressed within strains that is neither genetically nor environmentally driven, and that slows adaptive change, enhances drift, and lowers population growth.

Material and methods

We conducted our experiments using a bacterial microfluidic system called mother machine (Wang et al. 2010) (Fig.1). This system allows tracking thousands of individual cells via time-lapse phase-contrast microscopic imaging. For each cell the lifespan (age at death), the timing and number of divisions, as well as the size and cell elongation (cell growth) is recorded throughout their lives. We then explored these basic demographic data by constructing age-specific matrix models (Leslie matrices) and computed their demographic parameters.

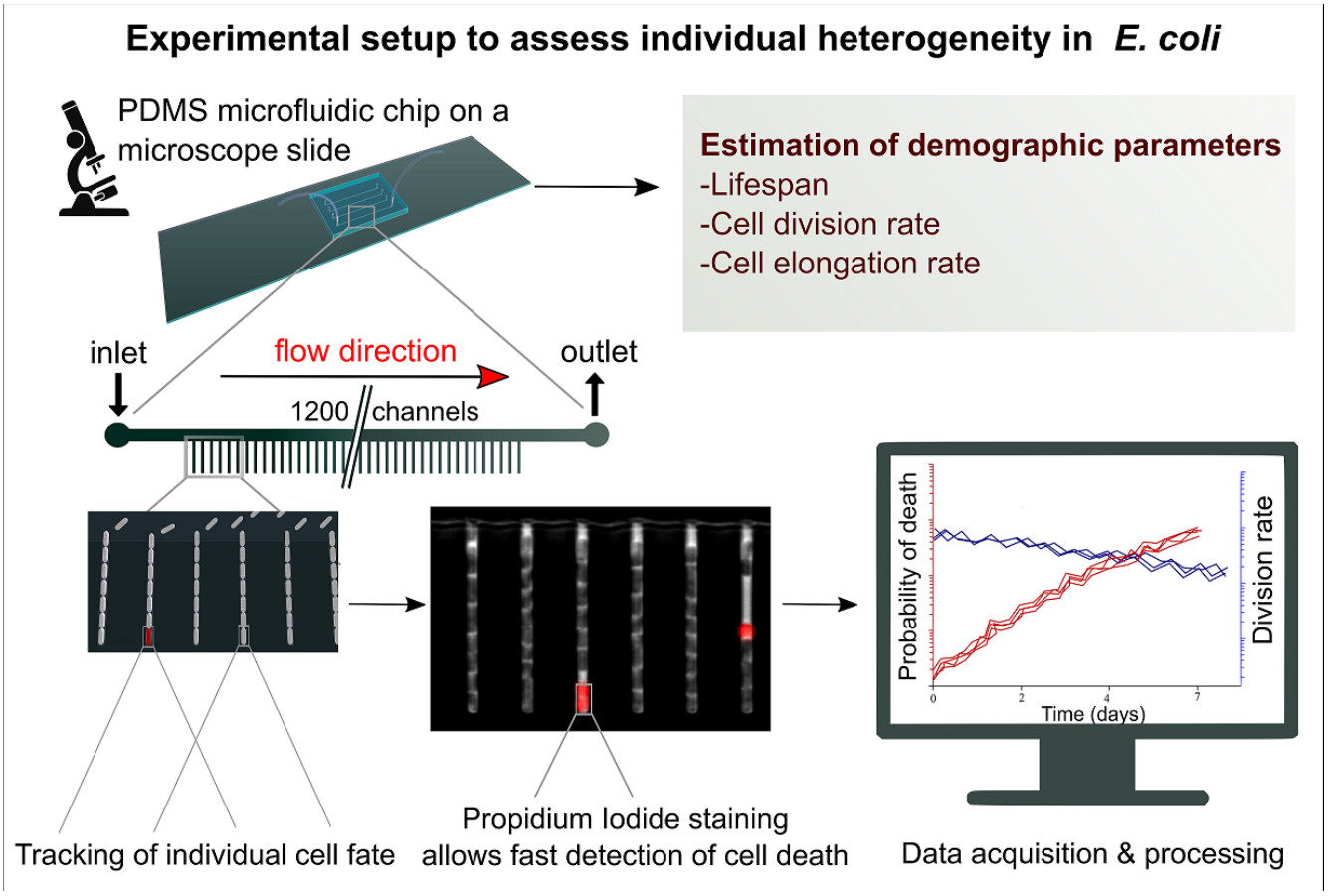

Fig. 1: Experimental setup of microfluidic system to track individual bacteria cells throughout their lifetime.

Microfluidic chip production

We started the replication of our microfluidic chips from a custom made (Sigatec SA) silicon (SiO) master. This silicon master in itself was first replicated in Smooth-Cast 310 and ONYX (Bentley advanced material) before we used this replicated mold to produce our PDMS chips (Sylgard Silicone Elastomer Base and Curing Agent mixed in 10:1 ratio). The PDMS chips were cured overnight at 75°C

in an incubator. We punched an inlet and outlet hole for the laminar flow in each chip using a sharpened 13 mm 22G Luer stub (Harvard Apparatus). Thereafter we bonded each PDMS chip on a glass cover slide (24×60 mm) after a 30 second air plasma treatment (PDC-002, Harrick Plasma). To load the chip with fluidics and to limit cell attachment to the PDMS surface, we activated the assembled chip for 18 seconds in air plasma, and immediately injected it with a 20% PEG (Polyethylene glycol) solution in filtered minimum bacteria growth media, M9, supplemented with 0.4% Glucose and 0.2% Casamino Acids (10 µM CaCl2, 200 µM MgSO4, 56 mM Glucose) (hereafter M9). We left the activated chip to incubate for a least 1 hour before we loaded bacteria into the chip.

Bacteria strains and loading of the microfluidic chip

We used seven strains of *E. coli.* Some of them are variants of the K12 strain MG1666 such as MG1655 (Hayashi et al. 2006), MG1655 LM (Hengge), and MG1655 (Inlag). The other K12 strains that we included were BW25113 (Datsenko and Wanner 2000), W3110 (Hayashi et al. 2006), and AB1157 (Bachmann 1972). To increase genetic diversity and include strains with different population growth rates in batch culture, we included the human commensal strain O8 IAI1 (Touchon et al. 2009).

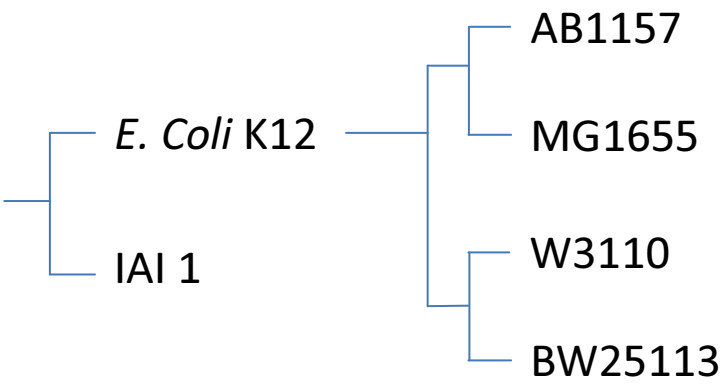

Fig. 2: Phylogenetic relationship among the different *E. coli* strains.

We plated the original bacterial stock suspension on a petri dish (LB + Agar) and then inoculated a single colony in LB (lysogeny broth) media grew it overnight, and stored it at -20°C in 20% glycerol suspension. From this stock we inoculated a fresh culture of the strain in 15ml of M9 in a 50ml tube, grown overnight. We then used 750µl of this fresh stock suspension to inoculate 75ml of M9, and let this solution grow at 37°C temperature until an OD600 of 0.4-0.6, which corresponds to exponential growth phase. We then centrifuged the bacteria suspension for 10 minutes at 4000rpm, we discarded the supernatant, and resuspended the cell pellet in 1ml fresh M9 media. We centrifuged the 1ml suspension again at 10000 rpm for 1 minute, discarded 800 µl of the supernatant, and resuspended the cell pellet in the remaining 200 µl M9. We then injected part of this concentrated cell suspension in the chip. We centrifuged the loaded chip at 350 rpm for 10min (~118g), reinjected concentrated cells and centrifuged again at the same speed to allow a high loading of the dead end side channels of our microfluidic chip where the rod-shaped bacteria cells grew. The focal cells were trapped at the end of these side channels, and we tracked the cells over their lifespan by time series imaging.

Life cell time series imaging

After we loaded the bacteria cells in the dead end side channels, we connected the chip to a peristaltic pump and placed the chip under an inverted microscope. We applied a continuous laminar flow (300µl/h) of M9 supplemented with 1.5% Polyethylene Glycol (PEG P3015 Sigma-Aldrich) and 1mg/ml PI (Propidium Iodide) through the main channel throughout the experiment (Fig. 1). For the life cell imaging, we defined 22-42 fields of view and a phase contrast as well as a fluorescent image was taken of each field of view at 4 minute intervals. Our Nikon Ti inverted microscope is equipped with a Perfect Focus System (PFS) that allowed us to maintain optical focus over the time series imaging. We used a 100× objective for the imaging and our microscope was controlled by Nis Element AR software. The microscope is temperature controlled at 37°C, in combination with the constant laminar flow we achieved highly controlled environmental conditions.

Image analysis

We analysed the time series images (4 min intervals) with customized application of Visiopales software. The software automatically detects each side channel, and uses a front detection to identify each cell within each side channel at each time point. We finally analysed the resulting raw data with custom developed R scripts (R Core Team 2016). The phase contrast images provided us with accurate data of the cell size and cell division (4 min intervals), while the fluorescence images provided us with accurate age at death information. When the cell wall lyses (cell dies) the PI bonds to the DNA and exhibits a strong red fluorescent signal.

Data analysis

We analysed the resulting demographic data, lifespan, cell elongation rate, cell division rate, of each focal cell. Since not all cells were dead at the end of the experiments we right censored these cells. Based on the individual cell demographic data we constructed Leslie matrix population models with one hour time intervals. We then used these Leslie models (one for each of the seven strains) to compute the following demographic parameters: the population growth rate, λ, the cohort generation time, T_c, the mean and among individual variance in lifespan, the mean and among individual variance in lifetime reproduction, the stable age distributions, and the age-specific reproductive values (Caswell 2001, Steiner and Tuljapurkar 2012, Steiner et al. 2014) (see Table 2, Supplementary material Appendix 1, Fig. A1, A2). We choose to estimate the mean and variance in fitness components – lifespan and reproduction – based on the Leslie matrix rather than on the original data to minimize the influence of different levels of right censoring. Fig. 3 shows the original observed data with the right censoring. Rates in Fig. 3 have been loess (program R) smoothed. To estimate the within strain variance in lifespan and reproduction and the among strain variance, we computed the mean variance within strains based on the seven measures of variances within each strain and related this mean variance to the variance in the means among the seven strains. Strain means and variances were equally weighted, i.e. we did not take into account that some means and variances were based on fewer cells compared to others. Our results are qualitatively robust to this assumption.

Results

Our results are based on a total of 3840 individual cells (3461 were tracked over their whole lifespan and 379 were right censored) (Fig. 3A,B). The cells in our experiments originated from seven isogenic strains (312 to 1017 cells per strain; mean 549 ± 189 SD) (Table 2). Population growth rates, λ, varied between 2.45 and 3.08 per hour (mean 2.88 ± 0.18 SD), mean lifetime reproductive success (net

reproductive rate, R_0) varied, between 49.57 and 134.16 individuals (mean 89.11 ± 23.91), generation time, T, varied between 1.51 and 1.79 hours (mean 1.58 ± 0.09 SD), and cohort generation time, T_C, varied between 25.2 and 61.8 hours (mean 44.9 ± 13.2 SD) (Table 2). The coefficient of variation in lifespan within strains (CV=within strain SD in lifespan/mean strain lifespan) varied between 0.72 and 1.46 (mean 1.01 ± 0.21), and was highly correlated to the CV of lifetime reproductive success within strains (0.76 to 1.44 (mean 1.02 ± 0.20)). Mean within strain variance in lifespan was high at 1630.85 h^2 compared to variance in mean lifespan among strains at 96.70 h^2. Similarly, mean within strain variance in lifetime reproductive success was high at 7847.73 ind^2 compared to variance in mean lifetime reproductive success among strains at 572 ind^2. Based on the variances within and among strains, ~94.4% of the variance in lifespan comes from within strains and 5.6% of variance in lifespan is caused by among strain variance. For lifetime reproductive success within strain variance dominates in generating ~93.2% of variance and 6.8% was observed among strains.

We illustrate the high variability in lifespan among individuals within strains in Fig. 3A. The corresponding age specific mortality patterns (Fig.3B) highlight the diversity in demographic patterns among strains. Such diversity is remarkable considering that all strains belong to the same species, *E. coli*, and have experienced identical constant environments throughout the experiments (highly controlled medium, nutrition, and temperature). Some strains show negative chronological senescence with declining mortality with increasing age (AB1157), others show more bathtub shapes with declining mortality early in life followed by classical senescence later in life (MG1655_LM, W3110), still others show only classical senescence with increasing mortality with age (BW25113), or finally others first show increased mortality early in life before exhibiting declining mortality later in life (MG1655, IAI1). Some of the late age mortality rates were estimated on small numbers of cells, and

the very old age patterns (e.g. MG1655-Inlag showing steep rising mortality again above 90h) should not be over-interpreted. We also reveal substantial among strain diversity in age specific division rates (Fig. 3C) and cell elongation rates (cell growth rates) (Fig. 3D). Most strains reach somewhat similar division rates after age 45h and show moderate decreases in division (reproductive senescence) at older ages. At younger ages division rates differ substantially among the different strains, by either being fairly constant or increasing with age. Cell elongation rates (cell growth grates) show similar diverse patterns among strains as mortality. Cell elongation (cell growth) increases (e.g. AB1157), decreases (e.g. IAI1), or first increases and then decrease (e.g. MG1655-Inlag) with increasing age. The age-specific reproductive values and stable stage distributions for the seven different strains are shown in the Appendix (Supplementary material Appendix 1, Fig. A1, A2).

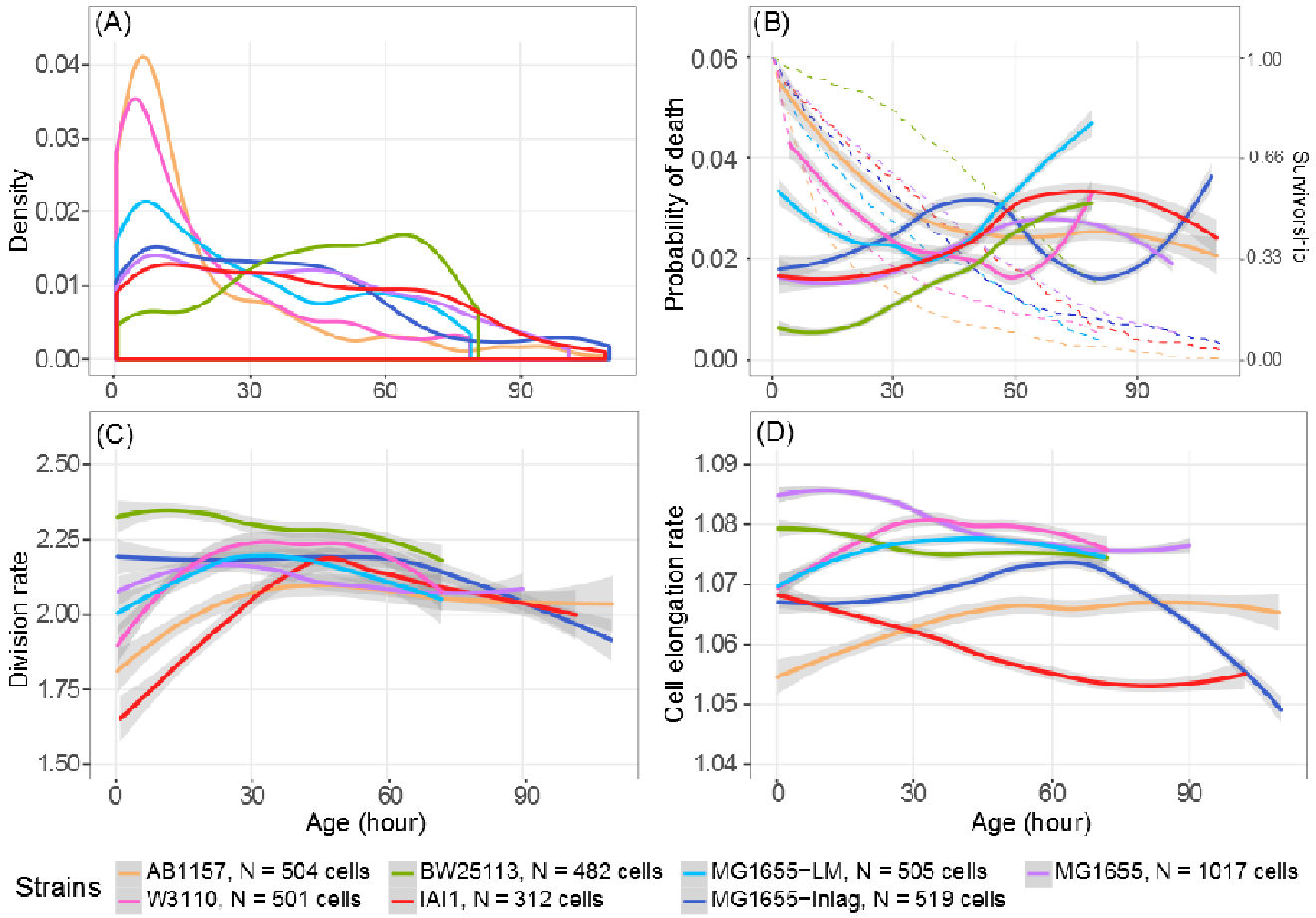

Fig. 3: Lifespan distribution (A), probability of death (B), division rate (C), and cell elongation rate (D) of seven different bacteria strains plotted against age in hours. For (B) also survivorship curves are plotted as dashed lines. 95 % CI are shown in grey shading (B, C, D). For B and C hourly rates are shown, for D rates per 4min intervals are shown. Note, cells of the different strains are truncated (right censored) at different ages.

Discussion

We show that fixed heterogeneity in lifespan and reproduction is fairly moderate compared to the heterogeneity among individuals within strains. Only our highly controlled study system allows such an accurate and direct decomposition of heterogeneity in genetic and neutral contributions. Under less controlled setting, as in natural populations, we would not have been able to decompose the causes of mortality and reproduction without bias (Steiner and Tuljapurkar 2012, Bonnet and Postma 2016, Cam

et al. 2016). Despite the dominating neutral variability within strains, we detected significant variability among strains. This selective difference is best illustrated by the differences in population growth rate, λ. These differences would lead to fast changes in genotype frequencies. Such fast evolutionary changes are due to our deliberate choosing of strains that were known to differ in their population growth rates in batch culture. The differences in λ directly inform us on each of the strains fitness, i.e. how fast the different strains would grow and compete against each other under the exponential growth conditions in our experiments. In our system, environmental conditions are such as to exclude any density dependence and promote exponential population growth as assumed under stable stage theories.

The within strain heterogeneity is partly illustrated by the coefficient of variation of the fitness components. The estimates we find here are comparable to less controlled systems and more complex organisms. In laboratory systems of other isogenic individuals under lab conditions the coefficient of variation (CV) ranges between 0.24 to 1.33 in lifespan [*Caenorhabditis elegans* 0.24-0.34 (Finch and Kirkwood 2000, Kirkwood et al. 2005), *Caenorhabditis briggsae* 0.31-0.51 (Schiemer 1982), *Saccharomyces cerevisiae* (0.37)(Kennedy 1994)]. Less genetically controlled lab populations do not differ much from these patterns in the CV of lifespan: laboratory reared mice (0.19-0.71)(Finch and Kirkwood 2000), *Drosophila melanogaster* 5.98-13.48 (Curtsinger et al. 1992). Even under less controlled conditions in the field, for instance, a plant species, *Plantago lanceolatum*, shows a CV 0.96 for lifespan, and 3.97 for reproduction (Steiner et al. unpublished) and such estimates seem not exceptional even in populations where we do not know the genetic or the environmental contributions (Tuljapurkar et al. 2009, Steiner et al. 2010). Even though in less controlled systems this CV includes contributions of fixed and dynamic heterogeneity and we cannot accurately decompose the neutral and selective variability as we unambiguously have done for our highly controlled bacteria setting, the

comparatively similar estimates between highly controlled lab systems and natural systems, might be seen as indicator that neutral variability might be substantial in natural populations. At least it is not unrealistic to assume such substantial neutral variability. One could also see it the other way around that our somewhat highly artificial and very simple model system might actually be not as different as one might at first assume, compared to more natural systems.

The ambiguity of estimates in natural populations about fixed and dynamic heterogeneity generating observed variances has resulted in a heated debate about neutral and adaptive contributions to this heterogeneity (Bonnet and Postma 2016, Cam et al. 2016). As with other neutral theories in molecular biology (Leigh 2007), or community ecology (Hubbell 2001), the neutral theory of life histories (Steiner and Tuljapurkar 2012) has been attacked based on a common misunderstanding behind neutral theories, that is, the erroneous claim that all variability is neutral. We know that all neutral theories are wrong (Leigh 2007). Any natural population includes selective differences, but the neutral theory illustrates to what extend heterogeneity might be neutral (in its theoretical extreme). To date, we do not have the means to unambiguously differentiate the causes driving the observed heterogeneity in natural populations. In our study here we show how substantial neutral heterogeneity might be, at least how large it is in this bacterial system. This large neutral heterogeneity might be surprising since the strains are highly adapted to the lab conditions. Selection has not managed to get rid of this variability, and we might have to ask how such neutral variability is maintained and if it is in itself adaptive.

Our results also illustrate how genetic variability, even within a species, can shape very diverse senescence patterns, both in survival and reproduction. Phylogenetically more closely related strains (Fig. 2) do not necessarily show more similar demographic patterns compared to less closely related strains (e.g. AB1157, MG1655, W3110). This raises interesting questions for comparative demography

where a single population of a species is frequently assumed to be representative for a whole species (Jones et al. 2014). Even under our highly controlled environmental condition we see great diversity in demographic patterns and it would be interesting to compare multiple natural populations of the same species to investigate how persistent demographic patterns within species are in nature.

One criticism on our data is that experiments are not entirely independently replicated. Each cell sits in its own little side channel, but the cells of each strain have still been loaded in the same microfluidic chip and are provisioned by the same highly controlled laminar flow. The amount of nutrients delivered to the cells is magnitudes larger compared to the amount all cells could ever possible consume; hence there should be no limitation of resources. We are convinced that our data is still representative since patterns among independent channels are highly replicable as we illustrate in the SM for one of our strains (Supplementary material Appendix 1, Fig. A3). High replicability has also been shown for other experiments with this system (U.K. Steiner unpublished).

Given the highly controlled environment and the high genetic control our system might also be predestined to investigate basic evolutionary theories of life history (Hamilton 1966, Stearns 1992). Such theories base much of their arguments on a fundamental tradeoff between reproduction and survival or early versus late life trade-offs. One of the challenges of assessing such trade-offs include that individuals, populations, or genotypes receive different amounts of resources (energy or nutrients) and these differences might override the underlying trade-offs (van Noordwijk and de Jong 1986). Our highly controlled environment and the clear distinction of genotypes might therefore provide a nice opportunity to reveal such tradeoffs that have been found hard to reveal in natural populations (Metcalf 2016). Based on the theories, we would predict that strains with high mortality should exhibit high reproduction (high division and cell growth rates). Such simple expectations are not met, strains with

relatively low mortality (e.g. BW25113) also show high cell elongation and division rates, while other strains show somewhat opposite patterns (e.g. AB1157). Similarly we do not detect clear age-specific trade-offs between early and late survival or early and late reproduction and their interaction as predicted by evolutionary theories of aging (Medawar 1952, Williams 1957, Hamilton 1966). Strain IAI1 for instance shows senescence in survival and in cell elongation rates, but increases in reproduction (division rate) with age, before plateauing off at old ages. Other strains (e.g. MG1655-Inlag) show increased and decreased mortality with age and similar patterns in cell elongation, but do not show much change in division rate over much of life. Only late in life does MG1655-Inlag, reveal some reproductive senescence. We can interpret the lack of such expected relationships among survival and reproduction as a lack of genetic linkage between traits and ages, and that the underlying tradeoffs are not as strong as assumed. We could also argue that this system is so artificial that we would not expect such trade-offs to be of any importance. Still, we see familiar demographic patterns even in this simple system, and we have to acknowledge that our best evidence for such trade-offs is coming from such artificial lab organisms, rather than from populations in their natural environments (Metcalf 2016). A fundamental challenge behind revealing these trade-offs is that they are expressed within individuals and not among individuals, but most of our attempts compare among individuals that belong to different groups, genotypes, populations, species, as we do in our study here.

In interpreting our results, we have to be aware that all strains are subjected to some level of right censoring (add exact numbers 1.4% to 26.3% mean 9.3% ± 8.8 SD). The number of individuals suffering from this censoring differs among the different strains and might therefore bias our results differently. We aimed at reducing the effect of the right censoring by estimating demographic parameters from Leslie matrices with open age brackets for the last age class.

Our findings unambiguously quantify fixed and dynamic heterogeneity for a simple bacterial system. We reveal that substantial neutral variability is generated by cell-intrinsic stochastic processes and that the quantity and timing of these processes differ among the clonal strains, shaping diverse age-specific demographic patterns. To what extends similar levels of neutral variability might be expressed in natural populations of simple organisms such as bacteria or more complex organisms has to be explored. We discuss similarities in coefficient of variation across different level in complexity among organisms and across levels of control that suggest that our results might not be so special. Promising attempts to overcome the unknown genetics of individuals in the wild have been made by releasing hundreds or thousands of genetically known crossed individuals into the wild and then tracked throughout their lives (Roach 2012, Travis et al. 2014). Evidence of such experiments suggests that levels of within cross heterogeneity is substantial compared to among cross heterogeneity, indicating substantial levels of neutral variability. How such neutral heterogeneity is maintained, how it has evolved, whether it is adaptive and if so under what conditions it is adaptive remains to be explored.

Acknowledgements

We thank all members of the Max Planck Odense Center on the Biodemography of aging for discussions and comments. We were supported by the Max Planck Society.

References

Ackermann, M. 2015. A functional perspective on phenotypic heterogeneity in microorganisms. - Nat. Rev. Microbiol. 13: 497–508.

Bachmann, B. J. 1972. Pedigrees of some mutant strains of Escherichia coli K-12. - Bacteriol. Rev. 36: 525–57.

Balázsi, G. et al. 2011. Cellular decision making and biological noise: from microbes to mammals. - Cell 144: 910–925.

Bonnet, T. and Postma, E. 2016. Successful by Chance? The Power of Mixed Models and Neutral Simulations for the Detection of Individual Fixed Heterogeneity in Fitness Components. - Am. Nat. 187: 60–74.

Cam, E. et al. 2016. The Conundrum of Heterogeneities in Life History Studies. - Trends Ecol. Evol. 31: 872–886.

Caswell, H. 2001. Matrix population models: construction, analysis, and interpretation. - Sinauer Associates.

Curtsinger, J. et al. 1992. Demography of genotypes: failure of the limited life-span paradigm in Drosophila melanogaster. - Science (80-.). 258: 461–463.

Datsenko, K. a and Wanner, B. L. 2000. One-step inactivation of chromosomal genes in Escherichia coli K-12 using PCR products. - Proc. Natl. Acad. Sci. U. S. A. 97: 6640–5.

Elowitz, M. B. et al. 2002. Stochastic gene expression in a single cell. - Science (80-.). 297: 1183–1186.

Endler, J. A. 1986. Natural selection in the wild (RM May, Ed.). - Princeton University Press.

Finch, C. and Kirkwood, T. B. 2000. Chance, Development, and Aging. - Oxford University Press.

Fitzpatrick, S. W. et al. 2016. Gene flow from an adaptively divergent source causes rescue through genetic and demographic factors in two wild populations of Trinidadian guppies. - Evol. Appl. 9: 879–891.

Hamilton, W. D. 1966. The moulding of senescence by natural selection. - J. Theor. Biol. 12: 12–45.

Hartl, D. J. and Clark, A. G. 2007. Principles of population genetics. - Sinauer.

Hayashi, K. et al. 2006. Highly accurate genome sequences of Escherichia coli K-12 strains MG1655 and W3110. - Mol. Syst. Biol. 2: 2006.0007.

Hubbell, S. P. 2001. The unified neutral theory of biodiversity and biogeography (SA Levin and HS Horn, Eds.). - Princeton University Press.

Jones, O. R. et al. 2014. Diversity of ageing across the tree of life. - Nature in press.

Kennedy, B. K. 1994. Daughter cells of Saccharomyces cerevisiae from old mothers display a reduced life span. - J. Cell Biol. 127: 1985–1993.

Kirkwood, T. B. L. et al. 2005. What accounts for the wide variation in life span of genetically identical organisms reared in a constant environment? - Mech. Ageing Dev. 126: 439–443.

Lande, R. et al. 2003. Stochastic population dynamics in ecology and conservation.

Leigh, E. G. 2007. Neutral theory: a historical perspective. - J. Evol. Biol. 20: 2075–91.

Lindner, A. B. and Demarez, A. 2009. Protein aggregation as a paradigm of aging. - Biochim. Biophys.

Acta 1790: 980–96.

Medawar, P. B. 1952. An unsolved problem of biology. - In: Uniqueness of the Individual. H. K. Lewis, in press.

Metcalf, C. J. E. 2016. Invisible Trade-offs: Van Noordwijk and de Jong and Life-History Evolution. - Am. Nat. 187: iii–v.

R Core Team, R. A. language and environment for statistical computing. 2016. R: A language and environment for statistical computing. (RDC Team, Ed.). - R Found. Stat. Comput. 1: 409.

Roach, D. A. 2012. Age, growth and size interact with stress to determine life span and mortality. - Exp. Gerontol. 47: 782–6.

Schiemer, F. 1982. Food Dependence and Energetics of Freeliving Nematodes. II. Life History Parameters of Caenorhabditis briggsae (Nematoda) at Different Levels of Food Supply. - Oecologia 54: 122–128.

Stearns, S. C. 1992. The evolution of life histories. - Oxford University Press Oxford.

Steiner, U. K. and Tuljapurkar, S. 2012. Neutral theory for life histories and individual variability in fitness components. - Proc. Natl. Acad. Sci. U. S. A. 109: 4684–9.

Steiner, U. K. et al. 2010. Dynamic heterogeneity and life history variability in the kittiwake. - J. Anim. Ecol. 79: 436–44.

Steiner, U. K. et al. 2012. Trading stages: life expectancies in structured populations. - Exp. Gerontol. 47: 773–81.

Steiner, U. et al. 2014. Generation time, net reproductive rate, and growth in stage-age-structured populations. - Am. Nat. 183: 771–783.

Touchon, M. et al. 2009. Organised Genome Dynamics in the Escherichia coli Species Results in Highly Diverse Adaptive Paths (J Casadesús, Ed.). - PLoS Genet. 5: e1000344.

Travis, J. et al. 2014. Chapter One – Do Eco-Evo Feedbacks Help Us Understand Nature? Answers From Studies of the Trinidadian Guppy. - In: Advances in Ecological Research. pp. 1–40.

Tuljapurkar, S. et al. 2009. Dynamic heterogeneity in life histories. - Ecol. Lett. 12: 93–106.

van Noordwijk, A. J. and de Jong, G. 1986. Acquisition and Allocation of Resources: Their Influence on Variation in Life History Tactics. - Am. Nat. 128: 137.

Vindenes, Y. and Langangen, Ø. 2015. Individual heterogeneity in life histories and eco-evolutionary dynamics (J-M Gaillard, Ed.). - Ecol. Lett. 18: 417–432.

Wang, P. et al. 2010. Robust growth of Escherichia coli. - Curr. Biol. 20: 1099–103.

Williams, G. C. 1957. Pleiotropy, Natural Selection, and the Evolution of Senescence. - Evolution (N.

Y). 11: 398.

Table 1: Notation and Equations

Description	Equation	Notes
	e_t	Vector of zeros with a 1 at position t (here t=1 for all estimations)
	e^T	Vector of ones, superscript T denote transpose
Identity matrix	$\mathbf{I}$	
Population projection matrix	$\mathbf{A}$	with $\mathbf{A} = (\mathbf{F} + \mathbf{P})$
Stage transition matrix	$\mathbf{P}$	Includes survival and stage changes
Fertility matrix	$\mathbf{F}$	
Population growth rate	λ =dominant Eigenvalue of $\mathbf{A}$	
Right eigenvector corresponding to dominant eigenvalue of $\mathbf{A}$	ω, normalized so to sum of components=1	
Left eigenvector corresponding to dominant eigenvalue of $\mathbf{A}$	υ, normalized so to $\upsilon_1 = 1$	
Generation time	$T = (\lambda * \upsilon * \omega)/(\upsilon * \mathbf{F} * \omega)$	
Stage duration matrix	$\mathbf{N} = (\mathbf{I} - \mathbf{P})^{-1}$	Elements quantify the expected time spent in each stage (at each age) conditional on the birth stage (here all individuals are born to stage 1= age 1)
Mean Lifespan	$exL = e^T * \mathbf{N} * e_t$	
	$exLsq = e^T * (2\mathbf{N} - \mathbf{I}) * \mathbf{N} * e_t$	

Variance in lifespan	$VarL = exLsq - (exL)^2$	
	$\hat{\mathbf{F}} = diag(\mathbf{F})$	Diagonal elements of fertility matrix (here first row fertility values)
Expected reproduction	$exR = {e_t}^T * \mathbf{F} * \mathbf{N} * e_t$	
	$exRsq = {e_t}^T * \mathbf{F} * (2\mathbf{N} - \mathbf{I}) * \hat{\mathbf{F}} * \mathbf{N} * e_t$	
Variance in reproduction	$VarexR = exRsq - (exR)^2$	
Cohort generation matrix	$\mathbf{A_c} = \mathbf{F} * \mathbf{N}$	
Right eigenvector corresponding to dominant eigenvalue of $\mathbf{A_c}$	$c\omega$, normalized so to sum of components=1	
Left eigenvector corresponding to dominant eigenvalue of $\mathbf{A_c}$	cv, normalized so to $(cv^T * c\omega) = 1$	
Cohort generation time	$T_c = (cv^T * \mathbf{N} * c\omega)/(cv^T * c\omega)$	

Details and proofs of equations are found elsewhere (Steiner et al. 2012, 2014)

Table 2: Key demographic parameters of the seven isogenic strains

Strain	λ	T	T_C	Lifespan	SD Lifespan	CV Lifespan	Mean LRS (R_0)	SD LRS (R_0)	# Individuals
AB1157	2.89	1.53	25.2	25	36	1.46	50	71	504
BW25113	3.08	1.53	61.8	57	51	0.90	134	121	482
O8 IAI1	2.45	1.79	55.5	44	32	0.72	87	66	312
MG1655 Inlag	3.06	1.51	43.8	43	38	0.87	94	80	519
MG1655 LM	2.97	1.53	34.1	32	36	1.12	70	82	505
W3110	2.91	1.55	38.8	36	40	1.11	78	88	501
MG1655	2.86	1.62	55.3	52	47	0.90	111	99	1017
									3840

Supplementary material Appendix 1

This contains the supplementary material for article “Demographic variability and heterogeneity among individuals within and among clonal bacteria strains” by Lionel Jouvet, Alexandro Rodríguez-Rojas, Ulrich K. Steiner

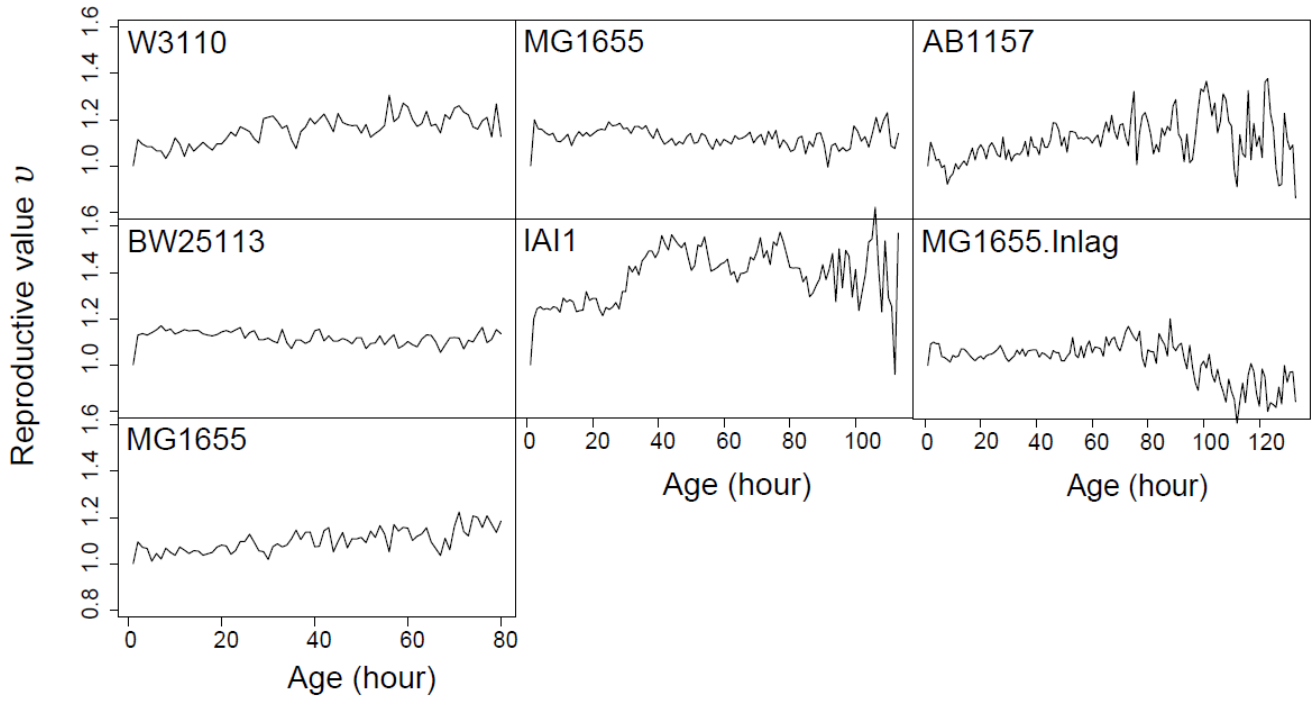

Fig. A1: Reproductive values, υ, across ages for the seven isogenic strains. Note, the x-axis are of different length according to right censoring, even though the distributions have been estimated based on the corresponding Leslie matrix for each strain and are hence not right censored.

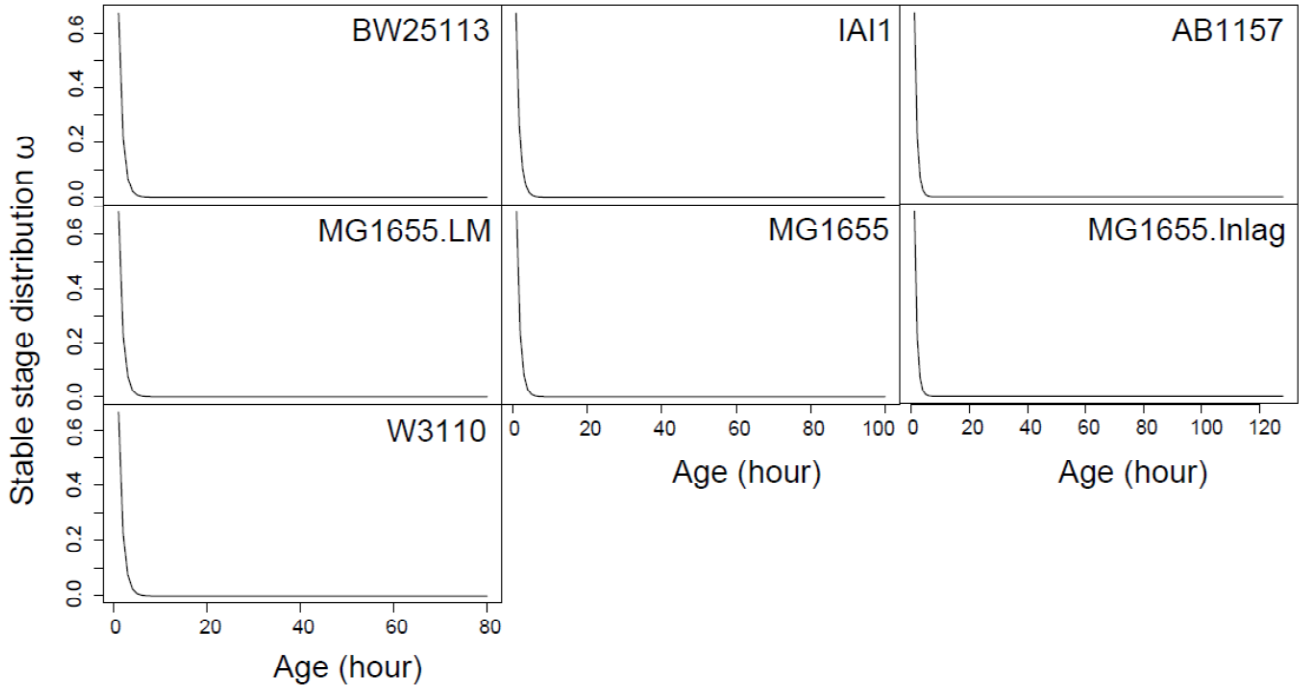

Fig. A2: Stable stage distribution, ω, describing the fraction of individual in each age class for the seven isogenic strains. Note, the x-axis are of different length according to right censoring, even though the distributions have been estimated based on the corresponding Leslie matrix for each strain and are hence not right censored.

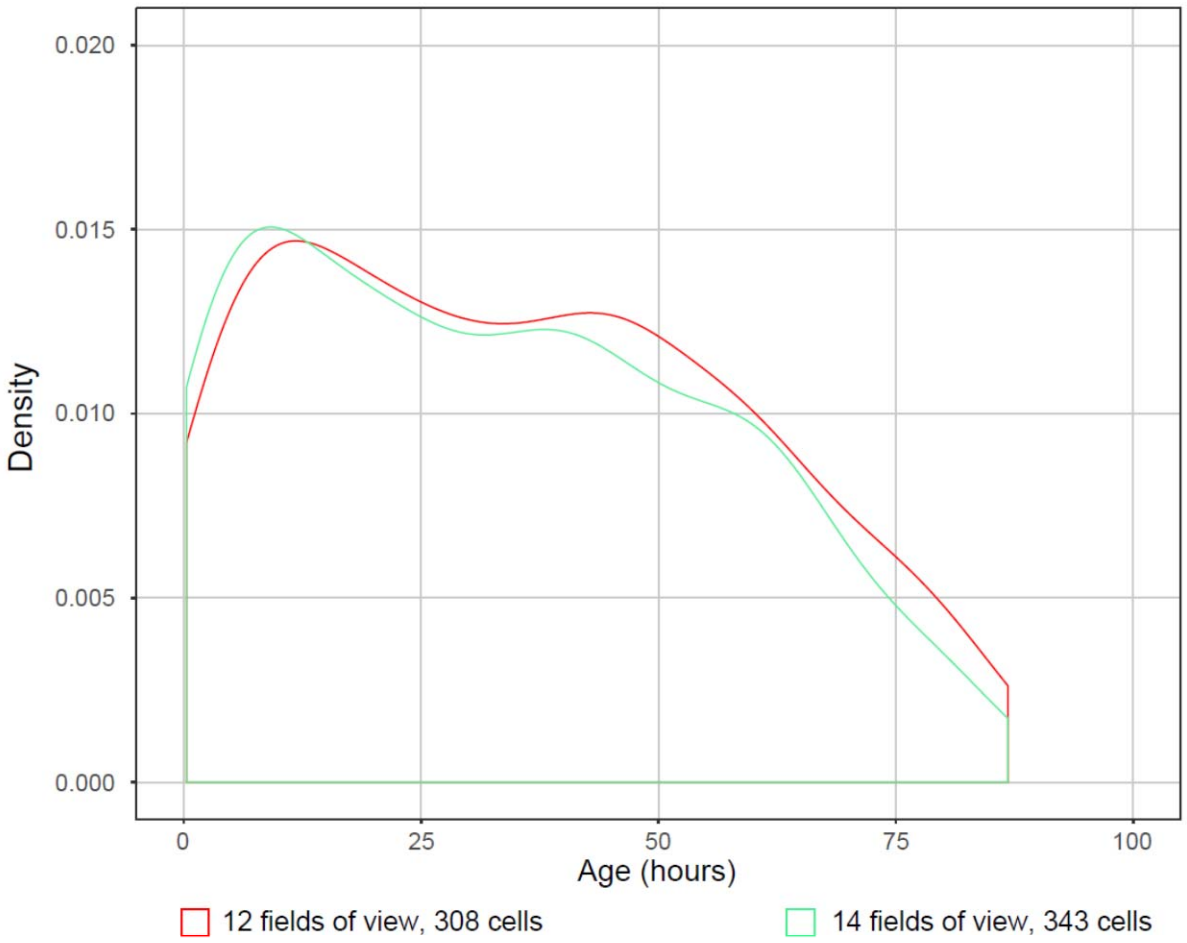

Fig. A3: Lifespan distribution of MG1655 cells replicated in two independent main channels.